Conf-941102--3

LA-UR-94-2018

Los Alamos National Laboratory is operated by the University of California for the United States Department of Energy under contract W-7405-ENG-36

TITLE: Waste Gas Combustion in a Hanford Radioactive Waste Tank

AUTHOR(S): J. R. Travis, R. K. Fujita, and J. W. Spore

SUBMITTED TO: American Nuclear Society
1994 Winter Meeting
November 13–17, 1994
Washington, D.C.

DISCLAIMER

Los Alamos National Laboratory
Los Alamos, New Mexico 87545

Waste Gas Combustion in a Hanford Radioactive Waste Tank

by

J. R. Travis, R. K. Fujita, and J. W. Spore
Engineering and Safety Analysis Group
Technology and Safety Assessment Division
Los Alamos National Laboratory

SUMMARY

It has been observed that a high-level radioactive waste tank generates quantities of hydrogen, ammonia, nitrous oxide, and nitrogen that are potentially well within flammability limits. These gases are produced from chemical and nuclear decay reactions in a slurry of radioactive waste materials. Significant amounts of combustible and reactant gases accumulate in the waste over a 110- to 120-d period. The slurry becomes Taylor unstable owing to the buoyancy of the gases trapped in a matrix of sodium nitrate and nitrite salts. As the contents of the tank roll over, the generated waste gases rupture through the waste material surface, allowing the gases to be transported and mixed with air in the cover-gas space in the dome of the tank.

An ignition source is postulated in the dome space where the waste gases combust in the presence of air resulting in pressure and temperature loadings on the double-walled waste tank. This analysis is conducted with hydrogen mixing studies (HMS),[1] a three-dimensional, time-dependent fluid dynamics code coupled with finite-rate chemical kinetics. The waste tank has a ventilation system designed to maintain a slight negative gage pressure during normal operation. We modeled the ventilation system with the transient reactor analysis code (TRAC),[2] and we coupled these two best-estimate accident analysis computer codes to model the ventilation system response to pressures and temperatures generated by the hydrogen and ammonia combustion.

Our analysis showed that the ventilation inflow temperature can significantly affect the mixing phenomena of the waste gases as they are released into the air dome space. There is essentially no mixing of the inflow air with the contents of the dome space when the inflow temperature is greater than the tank dome space average temperature.

We found that unfiltered waste gases can escape to the atmosphere at two different times during an accident sequence. First, during the release of the waste gases to the dome space, the tank pressure increases above the atmospheric pressure because the ventilation system cannot maintain the negative gauge value. This causes a flow reversal in the ventilation inflow riser. From this result, the Hanford project now designs filtration systems for the ventilation inflow ducts. Second, after the waste gas release phase, the mixture is ignited, and over the next second most of the

hydrogen and ammonia is oxidized with nitrous oxide as a waste gas component and the oxygen in the air, resulting in a pressure loading that rises to its maximum value. Structural damage may occur to the tank and ventilation system, such as loss of filtration, during this burn phase. As the tank depressurizes, the outflow of combustion product gases to the atmosphere through the ventilation exhaust and inflow ducts is unfiltered.

REFERENCES

1. T. L. Wilson and J. R. Travis, "Hydrogen Mixing Studies (HMS): Theory and Computational Model," Los Alamos National Laboratory report LA-12459-MS (December 1992).

2. K. O. Pasamehmetoglu, "TRAC-PF/MOD2: Vol. 1, Theory Manual," Los Alamos National Laboratory draft, Group TSA-6 report unnumbered.

DRAFT

WASTE GAS COMBUSTION IN A HANFORD RADIOACTIVE WASTE TANK

by

J. R. Travis, R. K. Fujita, and J. W. Spore

Engineering and Safety Analysis Group
Technology and Safety Assessment Division
Los Alamos National Laboratory

ABSTRACT

It has been observed that a high-level radioactive waste tank generates quantities of hydrogen, ammonia, nitrous oxide, and nitrogen that are potentially well within flammability limits. These gases are produced from chemical and nuclear decay reactions in a slurry of radioactive waste materials. Significant amounts of combustible and reactant gases accumulate in the waste over a 110- to 120-d period. The slurry becomes Taylor unstable owing to the buoyancy of the gases trapped in a matrix of sodium nitrate and nitrite salts. As the contents of the tank roll over, the generated waste gases rupture through the waste material surface, allowing the gases to be transported and mixed with air in the cover-gas space in the dome of the tank.

An ignition source is postulated in the dome space so that the waste gases combust in the presence of air, resulting in pressure and temperture loadings on the double-walled waste tank. This analysis is conducted with hydrogen mixing studies (HMS), a three-dimensional, time-dependent fluid dynamics code coupled with finite-rate chemical kinetics. The waste tank has a ventilation system designed to maintain a slightly negative gauge pressure during normal operation. We modeled the ventilation system with the transient reactor analysis code (TRAC), and we coupled these two best-estimate accident analysis computer codes to model the ventilation system response to pressures and temperatures generated by the hydrogen and ammonia combustion.

INTRODUCTION

The analytical tools used to model Hanford Tank 101-SY above waste surface phenomena were the coupled hydrogen mixing studies (HMS)[1] and transient reactor analysis code (TRAC)[2] computer codes. HMS is a finite-volume computer code that

$$\frac{\partial \rho}{\partial t}(\rho \mathbf{u}) + \nabla \bullet (\rho \mathbf{u}\mathbf{u}) = -\nabla p + \nabla \bullet \tau + \rho g\,, \tag{2}$$

where p is the pressure, τ is the viscous stress tensor, and g is the gravitational vector. The viscous force, $\nabla \bullet \tau$, is the usual Newtonian one. The mixture internal energy density equation is

$$\frac{\partial}{\partial t}(\rho I) + \nabla \bullet (\rho \mathbf{u} I) = -p\,\nabla \bullet \mathbf{u} + \nabla \bullet \mathbf{q} + Q\,, \tag{3}$$

where I is the mixture-specific internal energy and Q is the energy source, or sink, per unit volume and time owing to combustion and energy exchange with the crust and tank walls. The energy flux vector, $\mathbf{q}$, is given by

$$\mathbf{q} = \phi \nabla T - \rho\,\gamma \sum_{\alpha} h_{\alpha} \nabla \left(\frac{\rho_{\alpha}}{\rho}\right), \tag{4}$$

where f is the apparent or turbulent conductivity, g is the apparent or turbulent mass diffusivity, and h_a is the enthalpy for species a.

The Species Transport Equations

The transport, or mass, equation of the individual species is given by

$$\frac{\partial \rho_{\alpha}}{\partial t} + \nabla \bullet (\rho_{\alpha} \mathbf{u}) - \nabla \bullet \left[\rho \gamma \nabla \left(\frac{\rho_{\alpha}}{\rho}\right)\right] = S_{\alpha}\,, \tag{5}$$

where r_a is the mass per unit volume (macroscopic density) of species a. The source or sink term, S_a, represents the species mass created or destroyed by chemical reactions. When this equation is summed over all species, the result is the mixture mass [Eq. (1)].

Constitutive Relationships

The specific internal energy of any individual species is directly related to the temperature through a constant coefficient of specific heat at constant volume. The total specific internal energy is then given by the sum of all of the species' internal energies multiplied by its mass fraction. The equation of state for the fluid pressure is given by the usual ideal gas mixture equation.

Heat-Transfer Relationships

The convective heat exchange between the burning gas mixture and the waste surface is given by Newton's heating and cooling law, where the heat-transfer coefficient is calculated according to a modified Reynolds analogy. This expression contains the wall shear stress, which is related to the fluid density and the wall shear speed. We are unable to resolve turbulent boundary layers near solid walls with any practical computing mesh, so we match our solution near solid boundaries with a turbulent law of the wall, modified for rough surfaces. When the local Reynolds number is small, the law-of-the-wall formulation is not valid; thus, we use a laminar formulation.

We model the radiation heat transfer from the flame in a relatively simple fashion. We assume that 15% of the total chemical energy of combustion is radiated[3] from a point source at the computational cell center. This energy is radiated spherically away from each computational cell where combustion occurs to solid surfaces such as the crust, with the appropriate geometric view factors.

Turbulence Modeling

We use a simple algebraic, or mixing length, model adapted from the approach of Launder and Spalding.[4] In this model, the turbulent viscosity is proportional to the product of the fluid density, turbulent kinetic energy, and length scale of the energy-carrying eddies. Also, it is often estimated that 10% or less of the mean flow energy is contained in the turbulent kinetic energy, and the length scale is usually set equal to 0.25 to 0.5 m (9.8 to 19.7 in.) for containment-type problems.

Chemical Kinetics

We use a one-step chemical kinetics model that oversimplifies the actual chemical processes. In this model, the only reactions modeled are

$$H_2 + N_2O \rightarrow H_2O + N_2 + 77.4 \text{ kcal/mole } H_2 \text{ consumed}$$

(which we call reaction a),

$$H_2 + 1/2\ O_2 \rightarrow H_2O + 57.8 \text{ kcal/mole } H_2 \text{ consumed}$$

(which we call reaction b),

$$NH_3 + 3/2\ N_2O \rightarrow 3/2\ H_2O + 2\ N_2 + 105.1 \text{ kcal/mole } NH_3 \text{ consumed}$$

(which we call reaction c),

$$NH_3 + 3/4\ O_2 \rightarrow 3/2\ H_2O + 1/2\ N_2 + 75.7\ \text{kcal/mole}\ NH_3\ \text{consumed}$$

(which we call reaction d).

The reaction rate in these equations is modeled by a modified Arrhenius law. The general expression for the reaction rates is

$$\dot{\omega}_a = C_a [H_2]^{fa} [N_2O]^{Oa} e^{(-E_a / RT)}, \quad (6)$$

$$\dot{\omega}_b = C_b [H_2]^{fb} [O_2]^{Ob} e^{(-E_b / RT)}, \quad (7)$$

$$\dot{\omega}_c = C_c [NH_3]^{fc} [N_2O]^{Oc} e^{(-E_c / RT)}, \quad (8)$$

and

$$\dot{\omega}_d = C_d [NH_3]^{fd} [O_2]^{Od} e^{(-E_d / RT)}. \quad (9)$$

where C_a through C_d are the pre-exponential coefficients or frequency factors and E_a through E_d are activation energies for reactions a through d, respectively. The fuel exponents, f_a through f_d, and the oxidizer or reactant exponents, O_a through O_d, are set equal to 1 for this application. The terms in [ ] represent concentrations in moles/m^3, R is the universal gas constant, and T is the local gas temperature.

The finite-rate chemical kinetics can then be written for the H_2/N_2O reaction as

$$-\frac{d[H_2]}{dt} = -\frac{d[N_2O]}{dt} = \dot{\omega}_a, \quad (10)$$

and for the H_2/O_2 reaction,

$$-\frac{d[H_2]}{dt} = -2\frac{d[O_2]}{dt} = \dot{\omega}_b, \quad (11)$$

and for the NH_3/N_2O reaction,

$$-\frac{d[NH_3]}{dt} = -\frac{2}{3}\frac{d[N_2O]}{dt} = \dot{\omega}_c, \quad (12)$$

and for the NH_3/O_2 reaction,

$$-\frac{d[NH_3]}{dt} = -\frac{4}{3}\frac{d[O_2]}{dt} = \dot{\omega}_d \,. \tag{13}$$

These equations are actually weighted by the reactant volume fractions so that there is a partitioning function of hydrogen reacting with the available oxygen and nitrous oxide. The chemical energy of combustion, Q_C, is computed as a source term for the energy equation [Eq. (B-3)] by

$$Q_c = 4.184 \bullet 10^{10}\left(77.4\ \dot{\omega}_a + 57.8\ \dot{\omega}_b + 105.1\ \dot{\omega}_c + 75.7\ \dot{\omega}_d\right). \tag{14}$$

We have not attempted to quantify the effects of chemical decomposition at elevated temperatures of any gas specie not consumed in the combustion process.

In practice, when solving the finite-rate chemical equations [Eqs. (10) and (13)], we implicitly solve for the fuel concentration when the fuel-oxidizer mixture is fuel lean and for the oxidizer or reactant concentration when the fuel-oxidizer mixture is fuel rich. This ensures that combustion components will never be driven negative regardless of the timestep size.

Flame Propagation Model

To define the flame interface, which is the region separating the unburned gases from the burned gases, we implement a modification of the induction parameter model suggested by Oran.[5,6] In fact, the model is reduced to tracking a flame interface very much like the VOF method used for resolving free boundaries.[7,8] The combustion parameter equation is

$$\frac{\partial F}{\partial t} + \mathbf{u} \bullet \nabla F = 0 \,, \tag{15}$$

where the combustion parameter, F, moves with the fluid. A zero value of F denotes unburned gases, while a value of one indicates burned gases. We assume that in computational cells in which F is between zero and one, when F becomes 1/2, the chemical kinetics described above are activated. By employing a Donor-Acceptor flux approximation,[9] the interface remains sharp with minimal numerical diffusion.

The HMS Computational Model

An abbreviated description of the computational model is given here; refer to Wilson[1] for the details. The solution algorithm follows the LANL ICE'd-ALE[10–14] methodology for solving multidimensional, time-dependent fluid flow equations. For example, a transient fluid-dynamics timestep is broken into three distinct phases, which are discussed below.

Explicit Lagrangian Phase

In this phase, the densities, velocities, and specific internal energy fields are updated by the effects of all chemical and physical processes. This phase includes combustion, heat transfer, body forces, and turbulence effects. This ICE'd-ALE algorithm differs from most ICE'd-ALE methods in that velocities are positioned at the center of the computational volume faces rather than positioned at vertices. Because we are interested only in the Eulerian solution of the flow equations, a full continuous rezone will always be applied (see the Rezone Phase below), and this Lagrangian phase is only an intermediate step toward the full solution. We are able to devise a more efficient solution procedure by using the computational-volume-faced velocities.

Implicit Pressure Iteration Phase

In this phase, an implicit evaluation of the time-advanced densities, velocities, pressure, and specific internal energy fields is achieved. The purpose of this phase is to allow calculations of low-speed (low Mach number) flows without any timestep restrictions from the fluid sound speeds. A Poisson-type pressure equation is derived from the finitedifference equations, and an efficient matrix solution algorithm, called the conjugate gradient method,[15] is used to solve for the field variables. This implicit solution of the pressure equation allows for greater efficiency than a purely explicit calculation with reduced timesteps. The numerical stability achieved permits pressure waves to traverse more than one computational cell in a timestep so that low Mach number flows can be calculated without undue computational penalty.

Rezone Phase

Phase 3 explicitly performs all the convective flux calculations for mass, momentum, and energy. This phase completes the Eulerian calculation and therefore completes a timestep. By dividing the solution algorithm into these three phases, analysts can use whatever advection or rezoning algorithm they wish. We have made use of the simple donor cell, interpolated donor cell, van Lear, and flux-corrected transport algorithms.[16–19]

TRAC MATHEMATICAL MODEL

The TRAC-PFl/MOD2 computer code solves the two-phase, two-fluid mass, energy, and momentum conservation equations in lumped-parameter and 1-, 2-, and 3D geometries. The code was originally developed for light-water reactor nuclear safety studies. It is directly applicable to the Hanford waste tank ventilation system owing to both its networking capability (i.e., linking together complicated piping networks with different and coupled components) and its fast running speed.

The TRAC Conservation Equations

A complete description of the conservation equations solved by the TRAC-PFl/MOD2 computer code can be found in Ref. 2. For the Hanford waste tank ventilation system, the conservation equations solved by TRAC are a reduced set. For example, liquid water conservation equations are not required for the ventilation system because there is no significant amount of water in the ventilation system. Therefore, the single-phase, 1D gas conservation equations are solved by TRAC for the ventilation system analysis:

Vapor Mass Equation

$$\frac{\partial \rho}{\partial t} + \frac{\partial \rho v}{\partial z} = 0 \tag{16}$$

Vapor Equation of Motion

$$\frac{\partial v}{\partial t} + v\frac{\partial v}{\partial z} = -\frac{1}{\rho}\frac{\partial p}{\partial z} - c_w v|v| + g \tag{17}$$

Vapor Energy Equation

$$\frac{\partial \rho e}{\partial t} + \frac{\partial \rho v e}{\partial z} = 0 \, , \tag{18}$$

where z is the spatial variable, e is the internal energy, c_W is a drag coefficient, and all other variables have the same meaning as in the HMS equations described above.

Because the ventilation system is modeled with TRAC, which cannot calculate combustion processes, we are not able to compute ignition of waste gas mixtures in the ventilation system that may propagate back to the tank.

HMS/TRAC Coupling

The ventilation system for Tank Farm 241 and Tanks 102- and 103-SY are simulated using TRAC, while Tank 101-SY is simulated in detail using the HMS computer code. Because of the nature of the tank behavior and the ventilation system behavior, it was necessary to couple the HMS and TRAC computer codes. This coupling was accomplished by forcing consistent boundary conditions to be imposed at the physical locations where the two computer models interacted. For this calculation, these locations were (1) where the ventilation ductwork leaves Tank 101-SY, and (2) at the inflow leakage paths above Tank 101-SY. At these locations, TRAC determined the velocity or volumetric flow rate leaving Tank 101-SY, while HMS determined the pressure and temperature in the vicinity of the exit or entrance to Tank 101-SY.

The sequence through which information was passed is:

1. At the beginning of a timestep, HMS would use the TRAC boundary condition velocities to advance the time and determine the new time pressure and temperature distribution within Tank 101-SY.

2. The new Tank 101-SY pressure and temperature distributions would be used as boundary conditions for TRAC, which would advance the ventilation system solution and determine now-time velocities into and out of Tank 101-SY, which would be used as boundary conditions for the next HMS timestep advancement.

This, of course, implies that the velocity boundary conditions used by HMS were one timestep behind the pressure and temperature distributions. This is assumed to be an insignificant integration error because, in general, when the velocities, presures, and temperatures were changing rapidly (i.e., during a burn), the timestep size was reduced to roughly 0.1 ms.

This coupling between HMS and TRAC was accomplished by deleting the main driver program in TRAC and replacing it with a subroutine that would run TRAC through its input, initialization, steady-state integration, transient timestep integration, or output phases, depending on a control flag that was passed into the subroutine. A standalone driver was written to advance TRAC through a series of simple tests to verify that the TRAC controller subroutine worked, that boundary conditions for pressure and temperature were correctly passed into TRAC, and that TRAC correctly returned the velocities HMS needed as boundary conditions.

After the standalone code had tested the TRAC controller subroutine, appropriate calls to the TRAC subroutine were added to HMS. Test calculations were performed again to verify that information was transferred correctly between the two computer

codes and to verify that the coupling was stable. The initial coupling logic in TRAC allowed the pressure and temperature boundary conditions to be passed into TRAC and stored in a TRAC PLENUM component. This proved to be unstable at large timestep sizes. With a PLENUM component, the pressure and temperature from HMS were used as an initial guess at the beginning of the time advancement, and TRAC would attempt to update the pressure and temperature in Tank 101-SY based on the flows into and out of Tank 101-SY. Because the TRAC PLENUM component did not include any burning models, the new time-estimated pressure and temperature for Tank 101-SY would not be consistent with the HMS calculation. This inconsistency was observed to drive oscillations and instabilities at relatively large timestep sizes. The TRAC input model and coupling logic were changed to use a BREAK component to store the boundary conditions from HMS. This resulted in improved stability and accuracy. The use of the BREAK component as the coupling component in TRAC forced the boundary conditions to be consistent, and the observed instabilities went away. All calculations reported in this report used the BREAK component coupling. With a BREAK component, the pressure and temperature are fixed as boundary conditions during the TRAC time advancement.

TRAC Ventilation System Model

The components used to model the ventilation system for Tank Farm 241-SY are given in Table I. The component type identifies a specific component model within TRAC that was used to simulate the portion of the ventilation system described under the component description heading. The component number is used to distinguish one component from another within the TRAC model. A noding diagram that illustrates how the components are connected together is given in Fig. 1.

A BREAK component in TRAC provides a pressure and temperature boundary condition for the numerical solution of the conservation equations. The flow rates into and out of this component are determined from the solution of the momentum conservation equation given the pressure boundary condition specified in the BREAK component. If flow is into a BREAK component, the density and specific energy inferred from the specified pressure and temperature are ignored as boundary conditions. However, if flow is out of a BREAK component, the pressure and temperature specified in the BREAK component are used to determine the density and energy of the fluid leaving the BREAK component from the ideal gas relations. The density and energy are used as boundary conditions in the mass and energy conservation equations.

For BREAK components 5 through 8, atmospheric pressure and temperatures are input as constant values that do not change throughout the analysis. BREAK components 101, 121, and 131 are used to store the Tank 101-SY pressure and temperature information obtained from HMS and therefore will change during the simulation as HMS calculates new pressures and temperatures for the tank. A FILL

TABLE I

COMPONENTS USED TO SIMULATE VENTILATION SYSTEM

Component Type	Component Number	Component Description
VALVE	1	Inflow leakage path to Tank 101-SY
VALVE	11	Pump riser flow path to Tank 101-SY
VALVE	4	Inflow leakage path to Tank 102-SY
VALVE	3	Inflow leakage path to Tank 103-SY
BREAK	6 and 8	Atmospheric boundary condition for Tank 101-SY
BREAK	5	Atmospheric boundary condition for Tank 102-SY
BREAK	7	Atmospheric boundary condition for Tank 103-SY
VALVE	94	Outflow connection from Tank 101-SY
VALVE	95	Outflow connection from Tank 102-SY
VALVE	93	Outflow connection from Tank 103-SY
BREAK	101	Tank 101-SY boundary conditions from HMS
BREAK	121	Tank 102-SY boundary conditions from HMS
BREAK	131	Tank 103-SY boundary conditions from HMS
PLENUM	102	Single control volume to represent Tank 102-SY
PLENUM	103	Single control volume to represent Tank 103-SY
TEE	105	Ductwork between Tanks 102- and 101-SY and fan
TEE	104	Ductwork between Tanks 103- and 101-SY
FILL	106	Fan boundary condition

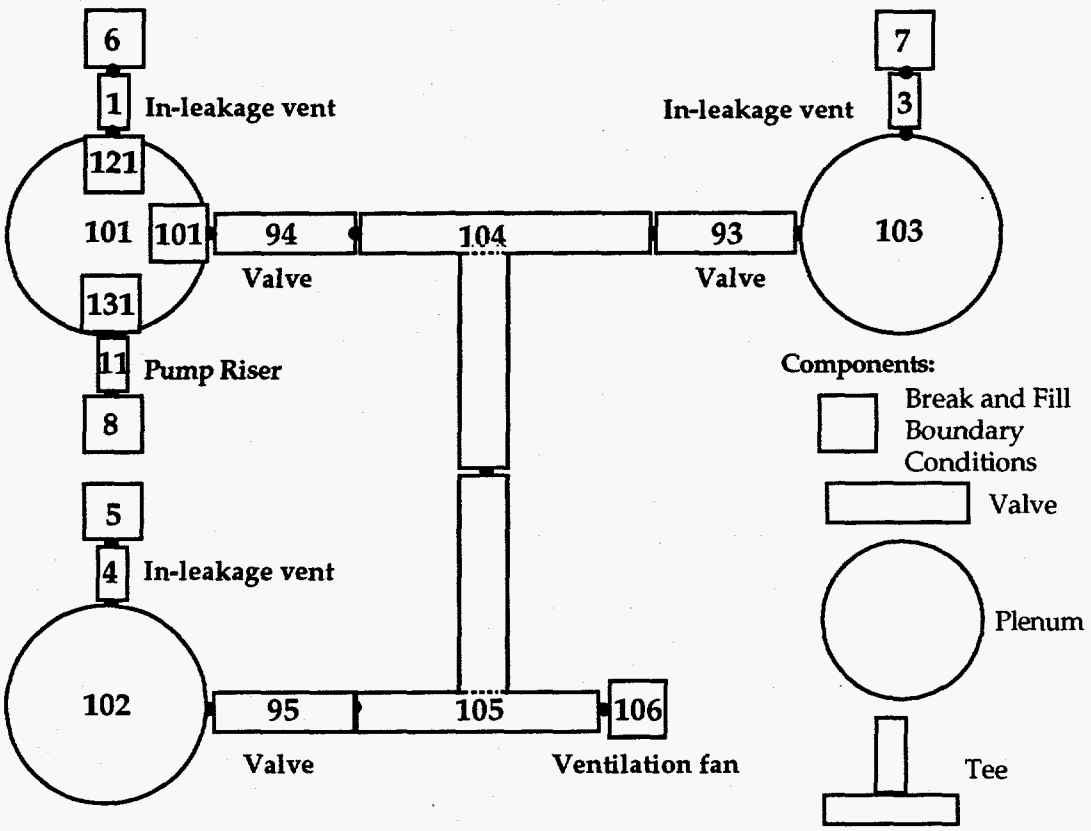

Fig. 1. TRAC noding diagram. Junctions (connecting labeled components) appear as small circles.

component in TRAC provides a flow rate boundary condition for the numerical solution of the conservation equations. The flow rate into a FILL component can be constant, a function of time, or a function of another variable in the TRAC simulation. To simulate the fan behavior, the flow rate in FILL component 106 was made a function of the fan head, which is the pressure difference between the first fluid cell upstream of the fan and the atmospheric pressure. Fan flow rate as a function of the fan head was supplied by WHC. These fan performance data were used as input to this model. For off-normal conditions, it was necessary to extrapolate the fan flow-rate-vs-head data. We assumed that at large velocities, the fan would fail. To estimate the hydrodynamic behavior of the failed fan, an effective flow resistance was estimated and used to extrapolate the fan flow rate-vs-head data into the high-velocity region.

VALVE components are essentially special piping or ductwork components that allow the user to change the flow area, i.e., the valve setting, at one location within

the component as the calculation is proceeding. As the flow area changes, the effective flow loss through the valve interface in the VALVE component changes based on experimental data for partially closed valves. The valve settings for VALVE components 1, 3, and 4 are adjusted to match the initial pressure in Tanks 101-, 102-, and 103-SY, respectively. The valve settings for VALVE components 94, 95, and 93 are adjusted to match the initial flow rates from Tanks 101-, 102-, and 103-SY, respectively. All six of these VALVE components contain two fluid cells, and the valve interface is the interface between these cells.

A TEE component can be used to represent the branching of a secondary set of piping or ductwork off of a primary set of piping or ductwork. The branching can be at any angle relative to the primary leg. The primary and secondary piping can be of varying and arbitrary diameters.

For TEE components 104 and 105, the piping is a uniform standard 0.3-m (12-in.)-diam schedule pipe. For these TEE components, the secondary-side piping is assumed to be 90 deg relative to the primary-side piping. The secondary-side piping for component 104 joins Tank 101-SY to the main ventilation line, and the secondary-side piping for component 105 joins Tank 102-SY to the main ventilation line. Tank 103-SY is joined to the main ventilation line by the first cell of the primary side of component 104.

A PLENUM component is a single control volume component that can have multiple inlet and/or outlet connections. A PLENUM component typically is used to represent a large volume, e.g., a waste tank, that has multiple piping connections to it. PLENUM components 102 and 103 are used to simulate Tanks 102- and 103-SY, respectively. Initial volumes, pressures, and temperatures are consistent with the conditions within Tanks 102- and 103-SY.

HMS Tank 101-SY Model

We have used both 3D Cartesian and cylindrical geometric representations of Tank 101-SY. To illustrate an HMS model and how it is coupled to the TRAC ventilation model discussed above, we will present the most coarse Cartesian geometry. This mesh is constructed of 7 equally spaced cells in the two horizontal directions and 5 equally spaced cells in the vertical direction, or 245 total computational cells. This mesh is shown in Fig. 2, with the dimensions given in meters. The crossed-out computational cells are internal obstacles that have been introduced to model the curvature of the tank's surfaces. In this coarse mesh, the stepping approximation to the curved surface is not good. Axial elevation level 2 is the same as 1, and axial elevation 4 is the same as 3. In axial elevation level 1, which is located just above the crust, we assume that the waste gases are released through approximately 60% of the waste surface area. This gas release area consists of cells in columns 4 through 7 and rows 1 through 7, as shown by the shaded area for level 1 in Fig. W-2. Axial

elevation 5 represents the top, or dome, of the tank, where the ventilation system is attached at the cell defined by row 3 and column 3 and designated B.

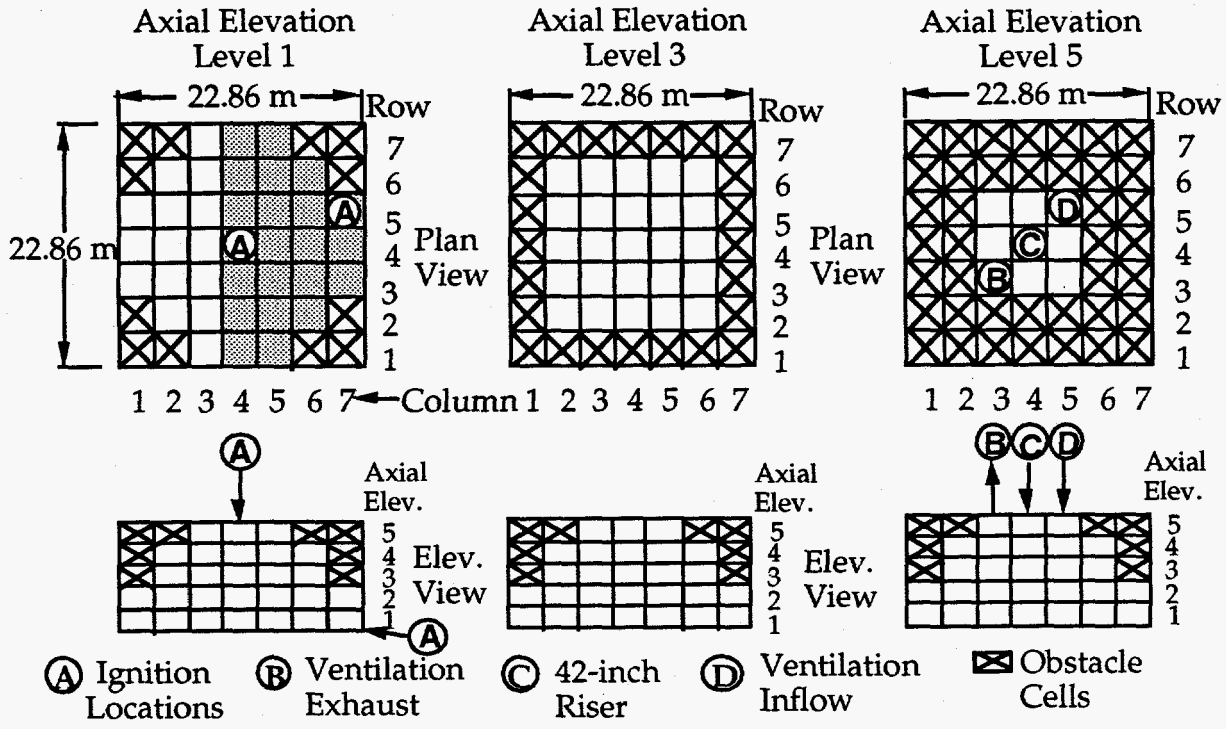

Fig. 2. HMS 7-X-7-X-5 Cartesian coordinate geometric model for Tank SY-101 showing relative positions of gas injection, tank ventilation connection, and tank in-leakage port.

In normal operation, the fan in the ventilation system draws a slightly negative gauge pressure on the tank, and filtered atmospheric air enters the tank through the ventilation inflow port shown at row 3 and column 5 cell and designated D. The center 42-in. riser is designated C and is shown in the center of the model at row 4 and column 4. Components 94, 11, and 1 of the TRAC model are connections B, C, and D, respectively. The appropriate area ratios are used between HMS and TRAC to ensure conservation properties.

Thermal-Hydraulic and Combustion Analysis

The thermal-hydraulic and combustion analysis simulated the injection and mixture of the release gases within the tank dome space, the combustion of the hydrogen, and the resulting gas transport through the leakage paths and ventilation system. The principal parameters of interest were the Tank 101-SY dome pressures and vapor temperatures. The pressure response of the tank was used as boundary conditions for the structural analysis of the tank.

The HMS/TRAC model assumed that the release gases entered the tank dome space through approximately 60% of the waste surface of the tank. All calculations considered hydrogen, nitrous oxide, ammonia, water vapor, and nitrogen as the release gas composition. The ignition of the released gases was initiated in a single cell located at two different locations. An ignition point at the top center of the dome space (see Fig. 2) was used for predictions that were to be used for structural analysis considerations because the top-down propagation of the flame front maximized the flame area and generally resulted in the highest tank peak pressures and pressure rise times for a given gas release volume. The other location for the gas ignition location was adjacent to the side of the tank on the surface of the waste.

Initially, a long-duration calculation without combustion was performed to determine the time at which maximum fuel concentration exists in the dome space. This calculation showed that the maximum concentration occurred 500 s after the initiation of a gas release. A typical HMS/TRAC calculation for a case with an operable ventilation fan consisted of a 30-s quasi-steady-state period to establish pressures and flows in the tanks and the ventilation system. This was followed by the 500-s release gas injection phase and then was followed with the hydrogen combustion phase. The calculation was continued until the tank pressure depressurized to atmospheric pressure. The accident sequences with the failed ventilation fan were run similarly except that the 30-s quasi-steady-state period was not used because the complete system was initialized to atmospheric pressure and thus did not require a steady-state initialization.

During operation of the pump, the tank is closed except for the ventilation system inflow and outflow port. It is during this normal operation that the tank faces a maximum expected gas release. Cases analyzed include the ventilation system

operable and inoperable and a top-down burn and bottom-up burn of the waste gases. Complete details of these calculations are presented in Ref. 20. The HMS/TRAC results for the dome pressure history following ignition for the top-down burn with the ventilation system inoperable are shown in Fig. 3. During the combustion phase, the peak dome pressure is 415 kPa (60 psia), and the peak temperature is 1480 K (2204°F). The top-down burn results in the shortest-duration pressure-rise times, which are of great concern in the structural integrity of the tank. For this case, we take credit for the waste having a certain amount of compressibility (there is an estimated 7540 ft^3 of retained gas in the waste at roughly 2.26 bar, which is the hydrostatic pressure at the bottom of the tank), and during combustion, one 42-in. riser initially begins to open when the tank pressure exceeds the pressure required to lift the riser cover off the riser-seating flange. The complete opening of the riser was determined by the equation of motion of the riser cover. The opening of the 42-in. riser reduces tank pressurization. The dome vapor space volume at the end of the gas release is 39,696 ft^3. This volume is dependent on the magnitude of the gas release because the greater the size of the gas release, the further the waste surface level drops, thereby increasing the dome space volume. The two bottom-up burn cases shown in Table III have higher peak pressures than the top-down burn case. However, the pressure-rise times for these two cases are less, so the structural consequences are less of a concern.[20] Therefore, the top-down burn case provides the bounding conditions for pump operation.

The bottom-up burn analysis resulted in the bounding radiological releases for this accident sequence, as shown in Table III.

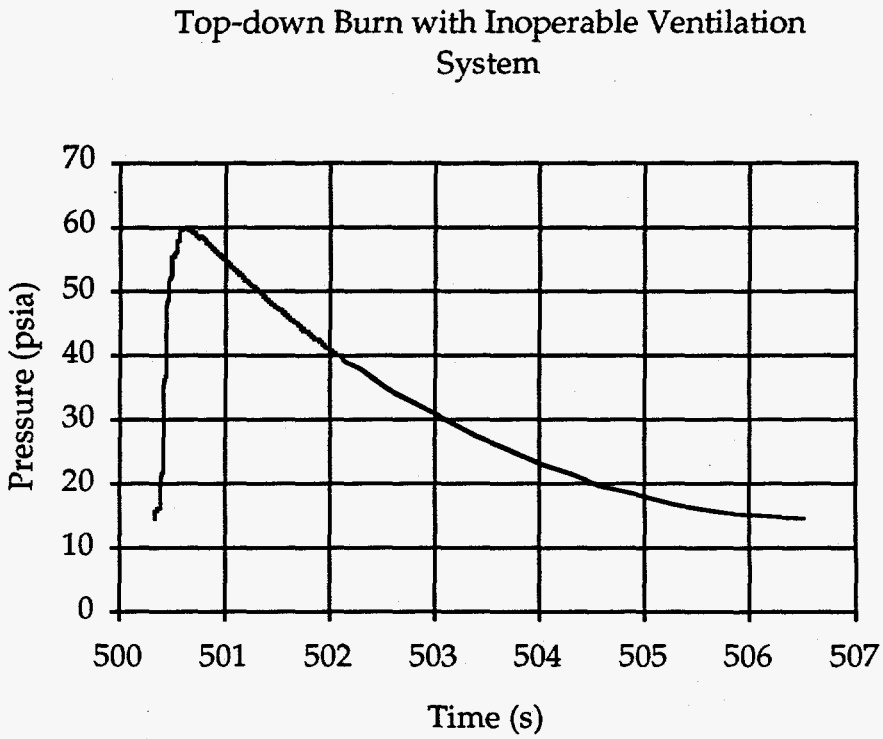

Fig. 3. Calculated tank dome pressure for pump operation—maximum expected release.

The toxicological consequences were also computed using the methodology described in Ref. 21. The resulting consequences are shown in Table IV. Using the worst-case ammonia releases in Table IV, ventilation inoperable and bottom-up burn, we compute a peak stack release rate of 11.50 g/s (0.025 lbm/s) and a peak ground release rate of 6.95 g/s (0.015 lbm/s). These consequences are computed to be 311 ppm onsite and 3.39 ppm offsite. The ammonia release rates are identical for both the top-down and bottom-up burn cases because the ammonia release rates are the maximum release rates predicted during the gas release phase of the calculation and thus are independent of the burn phase. The other cases considered for the Pump Operation—Maximum Expected Release are bounded by these conditions, as shown in Table III. The operation of the ventilation system for the top-down burn analysis had an insignificant effect on peak pressures and temperatures. The toxicological consequences were slightly less conservative than for the bottom-up burn with an operable ventilation system.

In Table V, we present for the bottom-up combustion cases an inventory of the gases contained in the dome vapor space before the burn phase. In addition, the burn time is given as the time from ignition to the maximum pressure.

TABLE III
THERMAL-HYDRAULIC RESULTS FOR THE HYDROGEN AND TOXIC GAS RELEASES DURING PUMP OPERATION—MAXIMUM EXPECTED RELEASES

Accident Sequence	Peak Pressure during Injection (psia)	Peak Pressure during Burn (psia)	Peak Temp. during Burn (°F)	Ammonia Released (g/s) Ground Release	Ammonia Released (g/s) Stack Release
Maximum expected release, top-down burn, ventilation not operable	15.0	60.5	2204	6.95	11.50
Maximum expected release, bottom-up burn, ventilation not operable	15.0	61.9	2276	6.95	11.50
Maximum expected release, bottom-up burn, ventilation operable	15.0	61.2	2258	6.30	11.80

TABLE IV
AMMONIA EXPOSURES (ppm) FOR THE HYDROGEN OR TOXIC GAS RELEASES DURING PUMP OPERATION

Accident Sequence	SY Farm	242-S Evap	U Plant	Hwy 240
Maximum expected release, top-down burn, ventilation not operable	311.25	106.97	34.84	3.39
Maximum expected release, bottom-up burn, ventilation not operable	311.25	106.97	34.84	3.39
Maximum expected release, bottom-up burn, ventilation operable	287.78	101.78	33.92	3.32

TABLE V
INVENTORY OF SPECIES GASES BEFORE IGNITION AND BURN TIME FOR BOTTOM-UP BURN

Accident Sequence	Inventory of Species (kg)					Burn Time (s)	Waste Mass Suspended (kg)	
	H_2	N_2O	N_2	O_2	NH_3		Total	Released
Maximum expected release, ventilation operable	6.1	114	820	229	25	0.24	2.13	1.69
Maximum expected release, ventilation not operable	6.2	116	822	230	25	0.23	4.64	3.32

REFERENCES

1. T. L. Wilson and J. R. Travis, "Hydrogen Mixing Studies (HMS): Theory and Computational Model," Los Alamos National Laboratory report LA-12459-MS (NUREG/CR-5948) (December 1992).

2. K. O. Pasamehmetoglu, J. W. Spore, and R. G. Steinke, et al., "TRAC-PFl/ MOD2: Vol. 1, Theory Manual," Los Alamos National Laboratory Group N-6 draft (November 1990).

3. R. Zalosh, Factory Mutual Corporation, personal communication, 1984.

4. B. E. Launder and D. B. Spalding, *Mathematical Models of Turbulence* (Academic Press, New York, 1972).

5. E. S. Oran, J. P. Boris, T. R. Young, M. Flanigan, M. Picone, and T. Burks, "Simulations of Gas Phase Detonations: Introduction of an Induction Parameter Model," Naval Research Laboratory memorandum report 4255 (June 1980).

6. E. S. Oran and J. P. Boris, "Weak and Strong Ignition. II. Sensitivity of the Hydrogen-Oxygen System," *Combustion and Flame* **48**, 149.

7. B. D. Nichols, C. W. Hirt, and R. S. Hotchkiss, "SOLA-VOF: A Solution Algorithm for Transient Fluid Flow With Multiple Free Boundaries," Los Alamos National Laboratory report LA-8355 (August 1980).

8. C. W. Hirt and B. D. Nichols, "Volume of Fluid (VOF) Method for the Dynamics of Free Boundaries," *J. Comp. Phys.* **39**, 201 (1981).

9. W. E. Johnson, "Development and Application of Computer Programs Related to Hypervelocity Impact," Systems, Science and Software report 3SR-353 (1970).

10. A. A. Amsden and C. W. Hirt, "YAQUI: An Arbitrary Lagrangian-Eulerian Computer Program for Fluid Flow at All Speeds," Los Alamos Scientific Laboratory report LA-5100 (March 1973).

11. J. D. Ramshaw and J. K. Dukowicz, "APACHE: A Generalized-Mesh Eulerian Computer Code for Multicomponent Chemically Reactive Fluid Flow," Los Alamos Scientific Laboratory report LA-7427 (January 1979).

12. A. A. Amsden, H. M. Ruppel, and C. W. Hirt, "SALE: A Simplified ALE Computer Program for Fluid Flow at All Speeds," Los Alamos National Laboratory report LA-8095 (June 1980).

13. L. D. Cloutman, J. K. Dukowicz, J. D. Ramshaw, and A. A. Amsden, "CONCHAS-SPRAY: A Computer Code for Reactive Flows with Fuel Sprays," Los Alamos National Laboratory report LA-9294-MS (May 1982).

14. A. A. Amsden, J. D. Ramshaw, P. J. O'Rourke, and J. K. Dukowicz, "KIVA: A Computer Program for Two- and Three-Dimensional Fluid Flows with Chemical Reactions and Fuel Sprays," Los Alamos National Laboratory report LA-10245-MS (February 1985).

15. R. Chandra, "Conjugate Gradient Methods for Partial Differential Equations," Ph.D. Thesis, Yale University (1978).

16. B. van Lear, "Towards the Ultimate Conservation Difference Scheme V. A Second-Order Sequel to Godunov's Method," *Comp. J. Phys.* **32**, 101 (1979).

17. J. P. Boris and D. L. Book, "Solution of the Continuity Equation by the Method of Flux-Corrected Transport," *Meth. in Comp. Phys.*, **16**, 85 (1976).

18. S. T. Zalesak, "Fully Multidimensional Flux-Corrected Transport Algorithms for Fluids," *J. Comp. Phys.* **31**, 335 (1979).

19. M. R. Baer et al., "A Two-Dimensional Flux Corrected Transport Solver for Convectively Dominated Flows," Sandia National Laboratories report SAND 85-0163 (1986).

20. R. K. Fujita and J. R, Travis, "HMS/TRAC Burn Analysis for Revision 8 of the Mixing Pump SA," Los Alamos calc note TSA6-CN-WT-SA-TH-029 (February 1994).

21. H. Sullivan, "A Safety Assessment for Proposed Pump Mixing Operations to Mitigate Episodic Gas Releases in Tank 241-SY-101: Hanford Site, Richland, Washington," Los Alamos National Laboratory report LA-UR-92-3196, Rev. 8 (March 8, 1994).